Elastic properties of magnetosome chains

2015 New J. Phys. 17 043007

(http://iopscience.iop.org/1367-2630/17/4/043007)

New Journal of Physics
The open access journal at the forefront of physics

Deutsche Physikalische Gesellschaft DPG
IOP Institute of Physics

Published in partnership with: Deutsche Physikalische Gesellschaft and the Institute of Physics

OPEN ACCESS

RECEIVED
22 December 2014

REVISED
6 March 2015

ACCEPTED FOR PUBLICATION
10 March 2015

PUBLISHED
8 April 2015

PAPER

Elastic properties of magnetosome chains

Bahareh Kiani[1], **Damien Faivre**[2] **and Stefan Klumpp**[1]

[1] Department Theory and Bio-Systems, Max Planck Institute of Colloids and Interfaces, Science Park Golm, D-14424 Potsdam, Germany
[2] Department Biomaterials, Max Planck Institute of Colloids and Interfaces, Science Park Golm, D-14424 Potsdam, Germany

E-mail: bahareh.kiani@mpikg.mpg.de

Keywords: magnetotactic bacteria, cytoskeletal filaments, bending stiffness, magnetic nanoparticles

Abstract

Magnetotactic bacteria swim and orient in the direction of a magnetic field thanks to the magnetosome chain, a cellular 'compass needle' that consists of a string of vesicle-enclosed magnetic nanoparticles aligned on a cytoskeletal filament. Here we investigate the mechanical properties of such a chain, in particular the bending stiffness. We determine the contribution of magnetic interactions to the bending stiffness and the persistence length of the chain. This contribution is comparable to, but typically smaller than the contribution of the semiflexible filament. For a chain of magnetic nanoparticles without a semiflexible filament, the linear configuration is typically metastable and the lowest energy structures are closed chains (flux closure rings) without a net magnetic moment that are thus not functional as a cellular compass. Our calculations show that the presence of the cytoskeletal filament stabilizes the chain against ring closure, either thermodynamically or kinetically, depending on the stiffness of the filament, confirming that such stabilization is one of the roles of this structure in these bacterial cells.

1. Introduction

The interior of living cells is highly structured, with membrane-bounded compartments providing functionally specialized chemical conditions and a cytoskeleton providing both mechanical stability and spatial organization [1]. For a long time, such spatial organization has been thought to be a hallmark of eukaryotic cells, but over the last two decades, it has become clear that structural complexity is not unique to eukaryotes, but rather that cytoskeletal structures as well as membrane-enclosed compartments also exists in bacterial cells [2, 3].

One particularly intriguing structure is the magnetosome chain of magnetotactic bacteria, a linear arrangement of magnetic nanoparticles that are enclosed in vesicles (magnetosomes) and aligned along a cytoskeletal structure, the magnetosome filament [4, 5]. The magnetic nanoparticles consist of magnetite (Fe_3O_4) or, in some species, greigite (Fe_3S_4) and have sizes in the range in which they are permanent magnets with a single magnetic domain [4]. The filament is built from an actin-related protein called MamK and the attachment of the magnetosomes involves linker proteins such as MamJ [6, 7]. The processes of biomineralization and of chain assembly appear to be tightly controlled and depend on a large number of different proteins [8, 9].

Thanks to the linear arrangement of the magnetosomes, the cells have a sufficiently large magnetic moment to be able to align with the magnetic field of the Earth, thus effectively using the magnetosome chain as a microscopic compass needle. Due to the alignment with the Earth field, the bacteria typically swim along the field lines, which is believed to facilitate the search for the preferred habitat, the oxic–anoxic transition zone in layered aquatic environments, due to the vertical component of the magnetic field of the Earth [4, 10, 11]. For the magnetosome chain to function as a compass needle, the linear arrangement of the magnetic nanoparticles is crucial as it provides a sufficient magnetic moment. Linear assemblies of magnetic nanoparticles have also received considerable interest in other fields including colloidal fluids [12, 13], nanomechanics [14], materials chemistry [15], and micro-swimmers [16]. A general problem with these systems is that chain-like assemblies of magnetic nanoparticles is limited and that chains often collapse into clusters and closed-ring structures [17]. In

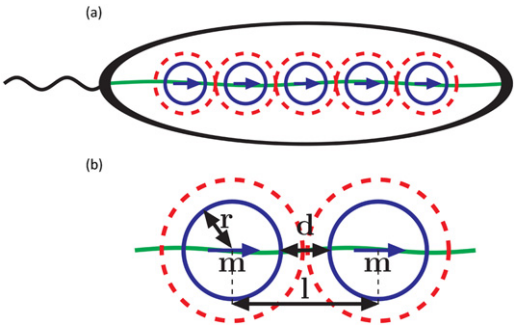

Figure 1. (a) Sketch of the magnetosome chain in magnetotactic bacterium: magnetic nanoparticles (blue circles) are attached to a cytoskeletal filament (green line), enveloped in membrane (red dashed lines). (b) Geometric parameters of magnetosome particles with radius r and magnetic moment $\mathbf{m}$.

magnetotactic bacteria, the filament is believed to provide mechanical support for such linear arrangement [7], but other roles have been proposed as well, such as a dynamic role in assembling and positioning the magnetosome chain during *de novo* chain formation and during cell division [18, 19]. Recent experiments also suggested that the connections with the magnetosome filament provides stability against intracellular torques due to moderately high magnetic fields [20]. In particular, the stability provided appears to exceed the stabilizing effect of the magnetic interactions between the magnetosomes.

In this study, we address a related problem, namely the bending stiffness of magnetosome chains. In electron microscopy images, magnetosome chains are typically rather straight. We specifically ask whether the bending stiffness is mostly due to the cytoskeletal structure or to the magnetic interactions, as magnetic particles are known to form linear structures [17, 21] without a stabilizing filament and (short) chains have been seen in cells lacking the MamK protein [22, 23]. To that end, we consider a model of (permanent) magnetic dipoles fixed on a semiflexible filament. We calculate the magnetic contribution to the bending rigidity and the persistence length and compare it with the contribution due to the filament. Previous studies have considered systems of this type either as chains of discrete particles [17, 21, 24] or as continuous magnetic rods [14, 25]. Here we follow the first route. For such systems, it is also known that magnetic particles form closed ring structures, so called flux-closure rings [26–28], thus we consider whether an actin-like semiflexible filament can stabilize a linear chain of magnetosomes against ring formation either thermodynamically or kinetically.

2. A model for the elasticity of magnetosome chains

To investigate the flexibility of a magnetosome chain, we describe it as a chain of permanent magnetic dipoles fixed along a semiflexible filament (figure 1). This magnetic and elastic energy is given by the dipole–dipole interactions between the magnetic dipoles and the bending elasticity of the filament,

$$E = E_{\mathrm{magn}} + E_{\mathrm{fil}}. \tag{1}$$

The magnetic contribution to the energy is given by

$$E_{\mathrm{magn}} = -\sum_{i=1}^{N}\sum_{j>i}^{N}\frac{\mu_0}{4\pi}\frac{1}{r_{ij}^3}\left(\frac{3(\mathbf{m}_i\cdot\mathbf{r}_{ij})(\mathbf{m}_j\cdot\mathbf{r}_{ij})}{r_{ij}^2} - \mathbf{m}_i\cdot\mathbf{m}_j\right), \tag{2}$$

where $\mu_0 = 4\pi\times10^{-7}\,\mathrm{N\,A^{-2}}$ is the vacuum permeability, the $\mathbf{m}_i$ are the dipole moments of magnetic dipoles and the $\mathbf{r}_{ij}$ are the distance vectors between them, with $r_{ij} = |\mathbf{r}_{ij}|$. In the following, we will assume that all dipoles have equal absolute value, $|\mathbf{m}_i| = m$. We will also take the distance between nearest-neighbor dipoles as constant, $r_{i,i+1} = l$, due to either the stiffness of the filament or due to steric constraints such as touching magnetosomes (figure 1(b)). We want to emphasize that mature magnetosomes are in the single-domain regime, i.e. they have permanent magnetic dipoles with rather large magnetization due to the absence of magnetic domains [29]. As a consequence, our model is considerably simpler than models for chains of superparamagnetic particles [30, 31], where the magnetization and thus the magnetic interactions depend on the external field experienced by the particle.

The elastic properties of the filament are described by a bending energy which is a quadratic function of the local curvature [32],

$$E_{\mathrm{fil}}\frac{\kappa_{\mathrm{fil}}}{2}\int_0^{L_{\mathrm{fil}}}\left(\frac{\partial \mathbf{t}}{\partial s}\right)^2 \mathrm{d}s. \tag{3}$$

Here s is a coordinate along the contour of the filament, $\mathbf{t}(s)$ is the unit vector along the tangent of the filament, and κ_{fil} is the bending rigidity. L_{fil} is the filament length, which we take to be equal to $L_{\mathrm{fil}} = Nl$.

3. Magnetic contribution to the elasticity

In this section, we consider the magnetic part of the energy function given by equation (2) separately, i.e. we omit the elastic contribution due to the filament and determine the sole contribution of the magnetic interactions to the elasticity of the chain.

3.1. Straight chain

We start by briefly considering the limiting case of a linear chain of magnetic dipoles. In the equilibrium state of such a chain, the dipoles orient parallel to each other and to the chain axis, thus the magnetic interaction energy is

$$E_{\mathrm{lin}} = -\sum_{i=1}^{N}\sum_{j>i}^{N}\frac{\mu_0}{4\pi}\frac{2\,m^2}{r_{ij}^3} = -N\epsilon\sum_{n=1}^{N-1}\frac{(1-n/N)}{n^3}. \tag{4}$$

In the last expression, we have introduced a characteristic energy scale $\epsilon = \frac{\mu_0}{4\pi}\frac{2m^2}{l^3}$, which represents the dipole–dipole interaction of neighboring dipoles in the chain. Nearest-neighbor interactions alone (given by the first term fo the sum, with $n = 1$) lead to $E_{\mathrm{lin}} = -N\epsilon\,(1 - 1/N)$. Due to the rapid decay ($\sim r^{-3}$) of the magnetic interactions, these nearest-neighbor interactions dominate the total energy. Indeed, for long chains ($N \to \infty$), the sum can be evaluated in terms of Riemann's zeta function as $\sum_{n=1}^{\infty} n^{-3} = \zeta(3) \simeq 1.2$, thus one finds that the full energy is only 20% larger than the nearest-neighbor contributions alone. We note that the parameter ϵ is related to the dipolar coupling parameter λ defined in earlier work [17] via $2\lambda = \epsilon/k_BT$ with the thermal energy k_BT, provided that the distance l is the minimal distance (i.e. when the magnetic particles or their non-magnetic coating touch each other).

Next, we give an estimate of the characteristic energy ϵ. For magnetite nanoparticles, the saturation magnetization (per volume) is $0.48 \times 10^6\ \mathrm{Jm^{-3}\,T^{-1}}$ [4]. For a particle of radius $r = 25$ nm, a typical value for magnetosomes in the well studied *Magnetospirilla* species [33], the magnetic moment is thus $m = 3.14 \times 10^{-17}\ \mathrm{JT^{-1}}$. The distance between neighboring magnetosomes can be estimated as $l = 2r + d \simeq 60$ nm, where $d \simeq 10$ nm is a gap distance between the magnetic particles accounting for the surrounding membranes. The characteristic energy ϵ is then estimated as $\epsilon \simeq 9.14 \times 10^{-19}\ \mathrm{J} = 221 k_BT$. This implies that the energy of a chain of 20 magnetosomes is $\simeq -2.0 \times 10^{-17}$ J or $-4900 k_BT$.

3.2. Bent chain

Next, we consider a bent chain and determine its bending rigidity and the corresponding persistence length. To that end, we consider a chain of dipoles on a (planar) circle with radius R. Thus two neighboring dipoles span a sector of the circle characterized by the bending angle $\varphi = 2\arcsin(\frac{l}{2R})$.

In addition to the assumption of equal magnetic moments, we now also assume that all dipoles have the same orientation with respect to the distance vector connecting them to their neighbor and characterize their orientation by the angle θ (figure 2). Since the magnetostatic interactions are short-ranged and dominated by the nearest-neighbor interactions, this assumption can be expected to be quite accurate except for the dipoles at the two ends of the chain. Minimization of the interaction energy with respect to θ leads to a tangential orientation of the magnetic moments, $\theta = -\varphi/2$.

The magnetic bending energy and thus the persistence lengths are obtained from a Taylor expansion of the energy in powers of l/R, i.e., for small curvature, which is described in the appendix. This calculation is similar to the calculation of the electrostatic persistence length of a polyelectrolyte [34]. If only nearest-neighbor interactions are included, the Taylor expansion leads to

$$E^{\mathrm{nn}} \approx -N\epsilon\left(1-\frac{1}{N}\right) + \frac{1}{8}N\epsilon\left(1-\frac{1}{N}\right)\left(\frac{l}{R}\right)^2. \tag{5}$$

Here the first term is the linear chain energy and the second term represents the contribution from bending with a magnetic bending rigidity of

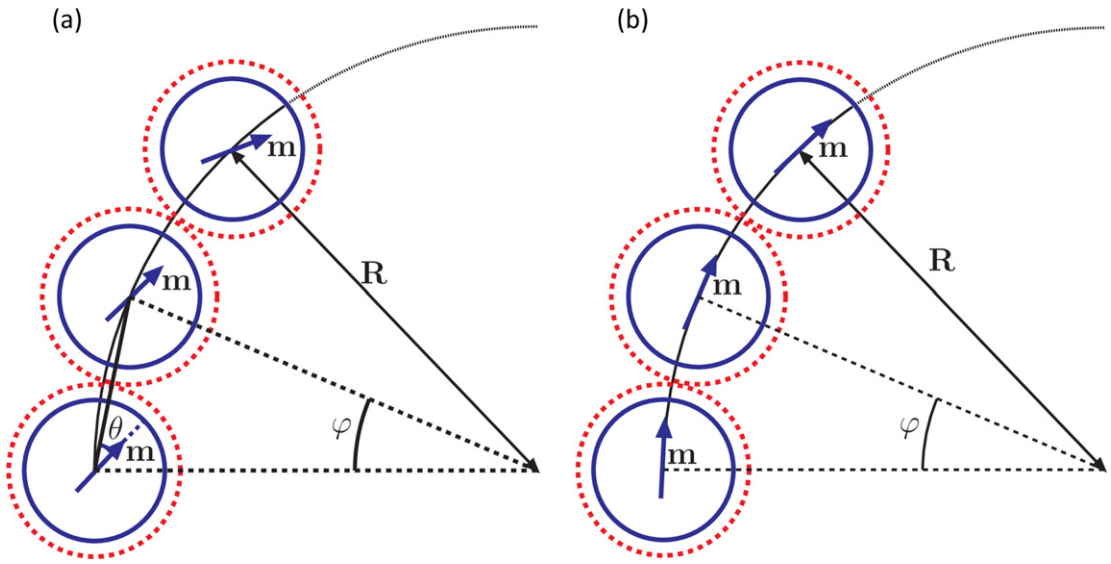

Figure 2. Bent magnetosome chain: (a) sketch of the geometry: the chain is bent onto a circle with radius R and a corresponding bending angle φ. The magnetic moments are oriented in an angle θ with respect to the line connecting neighboring magnetosomes. (b) In the equilibrium configuration, $\theta = -\varphi/2$, i.e., the magnetic moments align tangentially on the bending circle.

$$\kappa_{\mathrm{magn}}^{\mathrm{nn}} = \frac{\epsilon l}{4}\left(1 - \frac{1}{N}\right). \tag{6}$$

The same calculation can be done when including all magnetic interactions, see the appendix. In this case, we obtain the magnetic bending rigidity as

$$\kappa_{\mathrm{magn}} = \frac{\epsilon l}{4}\sum_{n=1}^{N-1}\frac{(1 - n/N)}{n^3} \approx \frac{\epsilon l}{4}\zeta(3) \simeq 0.3\epsilon l. \tag{7}$$

As the sum in this expression is the same as in the expression for the energy of a linear chain, the bending energy is also dominated by the nearest-neighbor interactions, with all other interactions contributing about 20% to the bending energy. We notice that our expression for the bending rigidity differs slightly, ≃14%, from a result reported in a recent study [35]. The two results show the same scaling behavior ($\kappa_{\mathrm{magn}} \sim \epsilon l$, but different numerical prefactors, $\zeta(3)/4 \simeq 0.30$ and $(\zeta(3) + 1/6)/4 \simeq 0.34$). In that study, the bending rigidity was derived from the energy difference between a straight chain and a closed ring. We will therefore come back to that discrepancy in the next section, where we discuss the closed-ring configuration.

Using a relation from polymer theory for semiflexible polymers [36], the bending rigidity can be converted into a persistence length,

$$\ell_{\mathrm{p,magn}} = \frac{\kappa_{\mathrm{magn}}}{kT} = \frac{\epsilon l}{4kT}\sum_{n=1}^{N-1}\frac{(1 - n/N)}{n^3}. \tag{8}$$

This parameter characterizes the length scale over which such a chain is straight under the influence of thermal fluctuations. Thus for the chain of magnetosomes considered above, we obtain a bending rigidity of 1.5×10^{-20} J μm or $3.7 k_B T$ μm. The corresponding magnetic persistence length at room temperature is 3.7 μm, which is comparable to the cell size (and longer than the typical chain length). Thus even due to the magnetic interactions alone, magnetosome chains in magnetotatic bacteria can be expected to be essentially straight. We note however that several studies have shown that the alignment of magnetotactic bacteria in external fields is subject to non-thermal fluctuations described by a substantially higher effective temperature [37, 38], likely induced by the motility of the cells. If bending of the magnetosome chain is subject to similar fluctuations, the thermal persistence length may overestimate the length over which magnetosome chains are straight in cells.

The magnetic energy scale ϵ is strongly dependent on the particle size, at least for particles in the single-domain size range (15–120 nm for magnetite [39]), where the magnetization is directly proportional to the volume and thus $\epsilon \sim r^6/(2r + d)^3$. As a consequence, the magnetic persistence length also increases strongly with particle size, as plotted in figure 3. We have plotted two cases in this figure: the circles are for magnetite particles that touch each other without gaps ($d = 0$), i.e. the distance between nearest neighbors is $l = 2r$. For the squares, we have taken the gap size $d = 10$ nm as constant to account for the presence of the magnetosome membrane around the magnetic particles. For example, a doubling of the particle size, compared to the case

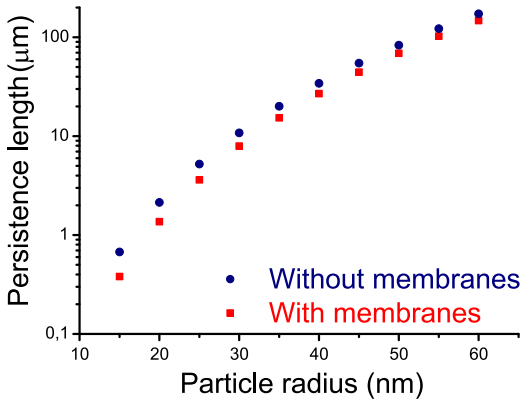

Figure 3. Persistence length as a function of particle size: values are calculated for a magnetosome chain of 20 spherical magnetite particles at minimal distances ($\ell = 2r + d$) with or without an enclosing membrane. Squares are for the case with a membrane of thickness 5 nm ($d = 10$ nm), circles for the case without a membrane ($d = 0$).

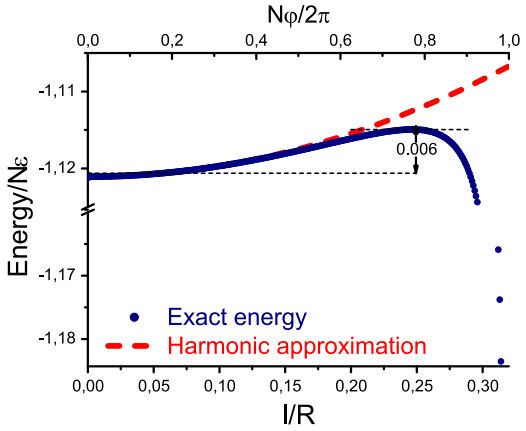

Figure 4. Magnetic energy of a chain as a function of the bending curvature given by the inverse of the ratio of the distance between nearest neighbors and the curvature radius (ℓ/R) or equivalently, the curvature angle φ (normalized to the angle for the closed ring configuration). The larger circle at the highest curvature shown indicates the closed ring configuration. The dashed line indicates the harmonic approximation, the arrows marks the barrier between the linear and close-ring configuration. The results shown here are for a chain of 20 particles.

considered above, leads to an increase of the magnetic persistence length to 65 μm. Particles of such size are found in some magnetotactic bacteria including in extraordinarily large cell of *Magnetobacterium bavaricum* (cell size ~10 μm and particles size 110–140 nm) [40]. On the other end of the size spectrum, for small magnetosomes with radius 15–20 nm, persistence length is about 1 μm, which is comparable with the chain length.

3.3. Closed-ring configuration

Figure 4 shows the full expression for energy as well as the harmonic approximation given by equation (21), as a function of chain curvature. Good agreement is seen for small curvatures, but for large l/R, the energy decreases again. In fact, the linear chain is not the configuration corresponding to the global energy minimum. The global energy minimum is found for a closed-ring configuration (also know as flux closure ring [41]), which has the maximal curvature possible. Assuming that the distance between neighboring magnetic dipoles is defined by steric constraints on the magnetosomes that the dipoles represent, the distance between the first and last particle (i.e.the dipoles with $i = 1$ and $i = N$) in the ring configuration will be l, i.e. the same as the distance of nearest neighbors in the interior of the chain. Thus, the closed ring is a configuration with the maximal bending angle $\varphi = 2\pi/N$, see figure 5 (larger angles would result in overlap of the first and last particle), and its equilibrium energy is given by

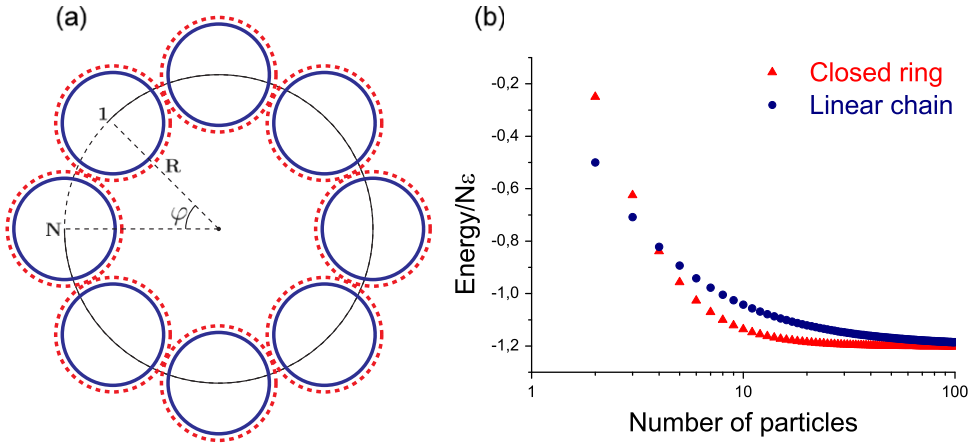

Figure 5. Linear and closed ring configurations of a chain of magnetic nanoparticles interacting only magnetically (no filament): (a) sketch of the closed ring geometry. (b) Magnetic energy for the linear and the closed-ring configurations as functions of the number of particles. The closed ring configuration has lower energy for chains with four and more particles.

$$E_{\mathrm{ring}} = -N\epsilon \sum_{n=1}^{N-1} \frac{(1 - n/N)}{4\left(\frac{\sin(n\pi/N)}{\sin(\pi/N)}\right)^3}\left(3 + \cos\frac{2\pi n}{N}\right). \tag{9}$$

That the closed ring is energetically favorable can be seen by the following estimate: the closed ring is stabilized by the additional nearest neighbor interaction between the first and last particle, which can be estimated as ϵ, but needs to overcome the bending energy, $\sim\epsilon/(8N) \times (Nl/R)^2 \sim \epsilon\pi^2/(2N)$. Thus, for sufficiently large N the interaction between the dipoles with $i = 1$ and $i = N$ overcompensates the effect of bending. This crude estimate indicates that the closed ring is the minimal energy configuration for chains of five or more particles, while a comparison of the exact energies for the linear chain and the closed ring (plotted in figure 5) shows that this is true for chains with four or more particles, as has already been shown in several earlier studies [17, 42–45]. We also note that the closed ring configuration with tangential orientation of the magnetization has been demonstrated experimentally using electron holography for cobalt nanoparticles [46]. For large N, the energy difference between straight chain and closed ring is small, as it decay as

$$E_{\mathrm{ring}} - E_{\mathrm{lin}} \approx -\frac{\pi^2\epsilon}{2N}\sum_{n=1}^{N-1}\frac{1 - n/N}{n^3}. \tag{10}$$

These considerations show that the relative stability of the straight chain and closed ring configuration depends not only on bending, but also on the additional interaction energies due to bringing the ends of the chain together. In a finite straight chain, the outermost particles contribute less to the total interaction energy than the particles in the chain interior, because of the smaller number of nearest neighbors, next-nearest neighbors etc. In the recent paper by Vella *et al* [35], the bending rigidity was calculated by identifying the bending energy with the energy difference between a closed ring of N particles and a straight chain of the same length, embedded within an infinitely long chain (and thus without finite size corrections to the energy). The rationale for this approach is that embedding has the same effect on the energy as ring closure and that in this way the contributions due to bending and due to ring closure can be separated. This approach is exact for the dominant nearest-neighbor interactions, and a good approximation for the full set of interactions. As mentioned, it leads to the same scaling behavior of the bending rigidity, but a slightly higher numerical prefactor. We note that, as the energy difference between ring and embedded chain reflects only bending and not ring closure, it cannot be used to determine the relative stability of these structures.

4. Including the filament

Now we include the elasticity of the filament and consider the full model with the energy given by equation (1). For the magnetosome chain on a circle with radius R, we can write the filament bending energy as $E_{\mathrm{fil}} = \kappa_{\mathrm{fil}} Nl/(2R^2)$. The total bending rigidity is obtained as the sum of the magnetic and elastic contributions,

$$\kappa = \kappa_{\mathrm{magn}} + \kappa_{\mathrm{fil}}. \tag{11}$$

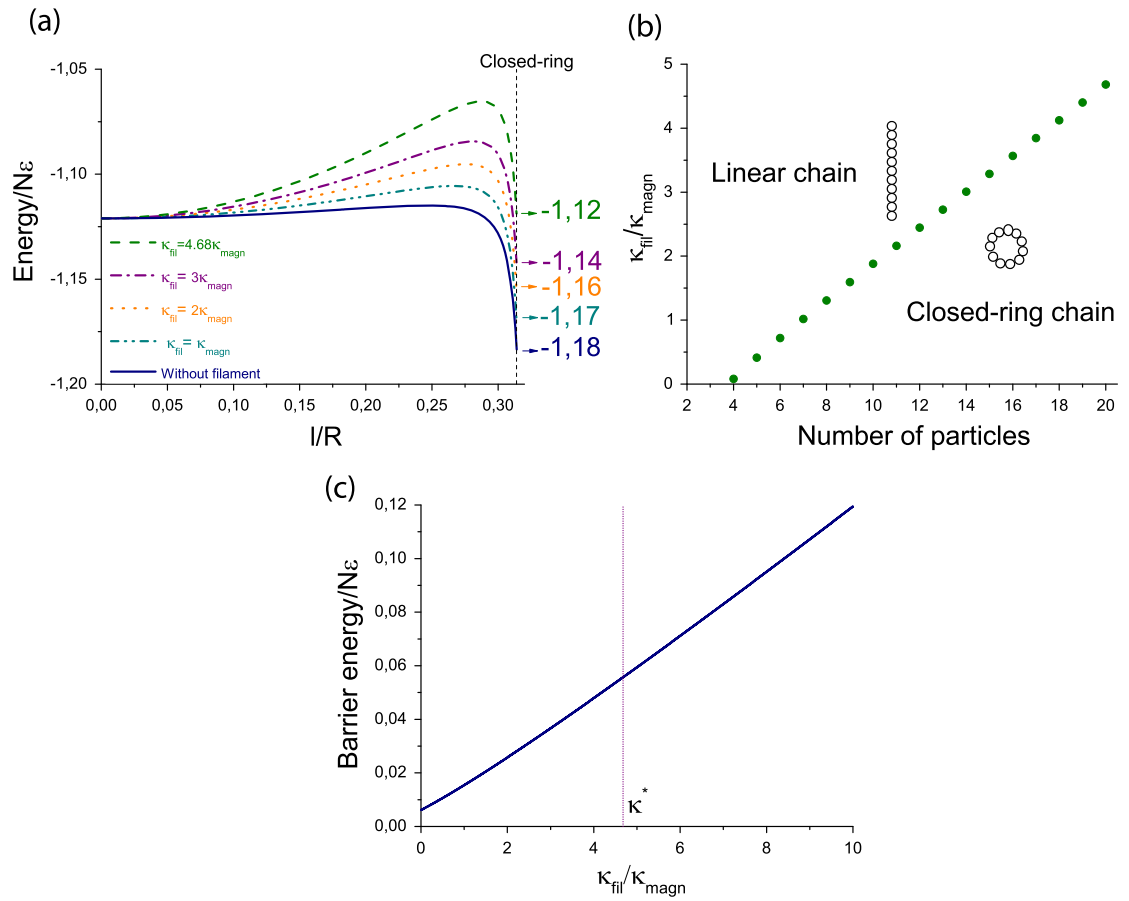

Figure 6. Bending of a magnetosome chain: (a) magnetic and elastic bending energy as a function of the curvature ℓ/R for different values of the filament bending stiffness $\kappa_{\rm fil}$. The uppermost curve is for the critical value of $\kappa_{\rm fil}$, for which the linear and the closed-ring configuration have the same energy. (b) State diagram indicating the lowest-energy configuration as a funciton of the ratio of the elastic and magnetic bending rigidities, $\kappa_{\rm fil}/\kappa_{\rm magn}$, and the number of magnetic particles. (c) Height of the energy barrier separating the linear-chain and closed-ring configuration as a function of the ratio of the bending rigidities. The vertical purple line indicates the critical bending rigidity, $\kappa^*_{\rm fil}$, above which the linear chain is the most stable configuration.

Likewise the persistence length of the magnetosome chain is also obtained by summing the two contributions, $\ell_{\rm p} = \ell_{\rm p,\ magn} + \ell_{\rm p,fil}$, and is thus essentially determined by the larger contribution. Above, we have estimated the magnetic persistence length for a typical magnetosome chain to be in the range of a few microns, with a strong dependence on particle sizes. The persistence length of a MamK filament is not known, but since MamK is a homolog of actin, we can compare this value with the persistence length of actin filaments, which has been measured to be 15–17 μm [47–49]. If we take this value as an estimate for the persistence lengths of the MamK filament, we can conclude that both contributions to the bending rigidity are of the same order of magnitude, but the filament contribution is the dominant one with $\kappa_{\rm fil}/\kappa_{\rm magn} \simeq 3$–5. However, this estimate is subject to some uncertainty, as the magnetosome filament may be a bundle of MamK filaments rather than a single filament and the details of its structure are unknown. Filament bundles can have even higher bending rigidities and persistence lengths; for example up to 100-fold larger bending rigidities have been reported for actin bundles, depending on the number of filaments in a bundle and the type of crosslinker [50]. Likewise, due to the strong dependence of the magnetic contribution part on size, the magnetic bending rigidity could be dominant in species with large particles.

As mentioned before, for chains with more than four magnetic particles the closed-ring configuration is more stable than a straight chain. Ring closure, however, does not confer any energetic advantage to the filament, only the cost due to bending, so the presence of the filament can be expected to stabilize the linear chain against ring closure. We thus ask whether the bending rigidity of an actin-like filament is sufficient to stabilize a linear magnetosome chain either thermodynamically, by making the linear configuration the global energy minimum, or kinetically, by increasing the energy barrier between the linear and the ring configuration. Figure 6(a) shows the total energy of the magnetosome chain as a function of curvature for different values of $\kappa_{\rm fil}$. One can see that both the energy of the closed ring and the height increase as the bending rigidity of the filament is increased. The dashed green line shows the case, where $\kappa_{\rm fil}$ is chosen such that the energy of the straight chain and of the closed ring are the same. This critical value $\kappa^*_{\rm fil}$ is given by

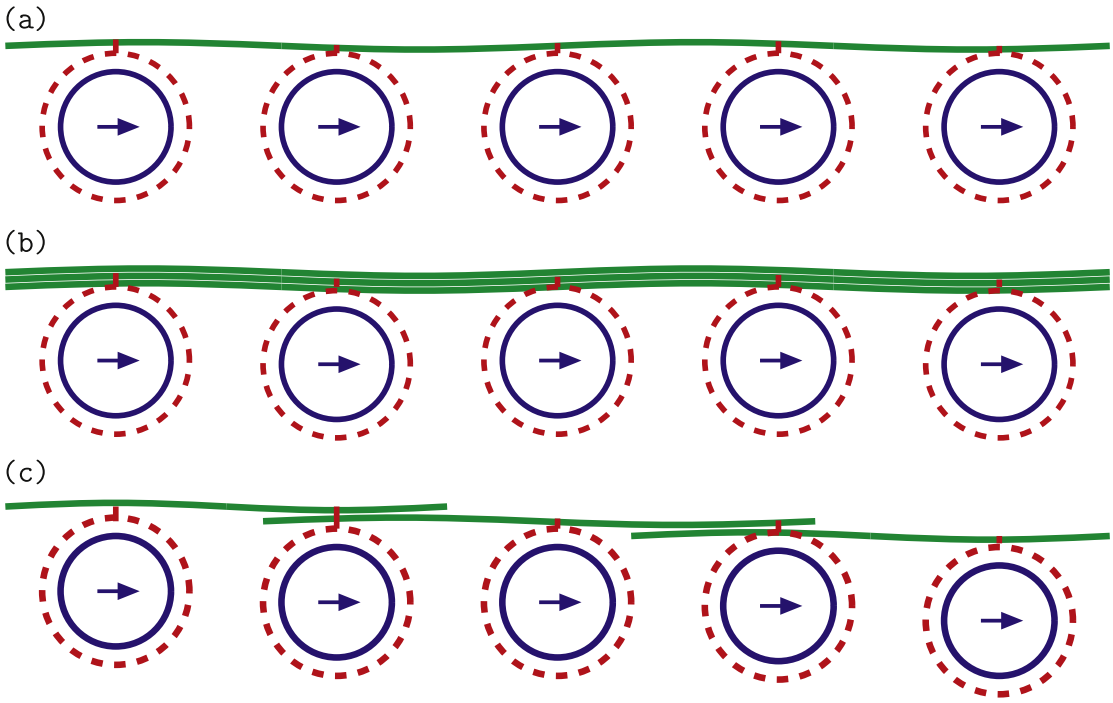

Figure 7. Schematic picture for possible structures of magnetosome filaments: (a) a single long filament extending from one cell pole to the other, (b) a bundle of long filaments, (c) a long bundle consisting of shorter filaments.

$$\kappa^{\star}_{\mathrm{fil}} = \frac{l\epsilon}{4\sin^2(\pi/N)}\left(\frac{\sin^3(\pi/N)}{2}\sum_{n=1}^{N-1}\frac{1-n/N}{\sin^3(n\pi/N)}(3+\cos(2\pi n/N)) - 2\sum_{n=1}^{N-1}\frac{1-n/N}{n^3}\right). \tag{12}$$

For a chain of 20 magnetosomes, this condition is met for $\kappa^{\star}_{\mathrm{fil}}/\kappa_{\mathrm{magn}} \simeq 4.68$. Calculating this critical value of κ_{fil} for different numbers of particles allows us to determine a morphological diagram as a function of the ratio of bending rigidities $\kappa_{\mathrm{fil}}/\kappa_{\mathrm{magn}}$ and the particle number. This diagram (figure 6(b)) exhibits two regimes, one in which the ring configuration is the globally most stable one and another where the straight chain is the most stable configuration. Not surprisingly, an increasing κ_{fil} extends the linear chain region.

Assuming a bending rigidity of the filament similar to a single actin filament will bring the system close to the transition, but typically the closed ring will still be the most stable configuration (for $\kappa_{\mathrm{fil}}/\kappa_{\mathrm{magn}} \simeq 4$ and $N \simeq 20$.) Thus, a bending rigidity only slightly higher than actin's (about 1.6-fold) or a small bundle of a few actin-like filament would stabilize the straight chain thermodynamically, i.e. making it the globally stable configuration. However, even lower values of the filament stiffness than for a single actin filament may have an important impact in the cell, as they are sufficient to destabilize small rings. Within the spatial confinement of the cell, small rings and clusters containing small rings may be the dominant competing assemblies as the confinement makes large rings are rather unlikely.

In addition, a ratio of the bending rigidities of $\kappa_{\mathrm{fil}}/\kappa_{\mathrm{magn}} \simeq 4$ leads to an increase in the barrier height of almost an order of magnitude (figure 6(a)), so that even lower filament bending rigidities should be sufficient to stabilize the linear configuration kinetically. In the cell, additional stabilization is provided by the confinement due to the cell's membrane, which will prevent large ring structures.

To summarize these considerations, figure 7 shows three possible structures of the magnetosome filament, a single filament spanning the whole cell, a bundle of filaments individually spanning the whole cell, and a bundle of shorter filaments. In the first case, the filament stabilizes the linear chain kinetically by increasing the barrier to ring closure, but most likely, the closed ring is still the configuration with the globally lowest energy. In the second case, the linear chain corresponds to the global energy minimum, and the third case remains somewhat unclear. As thermodynamic stabilization requires a filament stiffness only 1.6-fold larger than actin's, such a bundle may be strong enough if the bundle consists of at least two filaments along its full length. On the other hand, such a structure may be locally less stiff and thus be prone to bending at specific points.

5. Concluding remarks

In this study, we have addressed the bending stiffness of magnetosome chains, which results from two main contributions, a magnetic one due to the magnetic interactions between magnetosomes that favor straight chain orientation, and an elastic contribution due to the bending stiffness of the actin-like cytoskeletal filament to which the magnetosomes are attached. Our analysis shows that while both contributions are relevant, the bending stiffness of the filament can usually be expected to be the dominant part, with an about four-fold longer persistence length than due to magnetic interactions alone. However, even the magnetic interactions alone can be expected to result in a straight chain, as the persistence length exceeds the chain length. This conclusion should however be taken with the caveat that it relies on the assumption of thermal fluctuations of the magnetosome chain, while at least for the alignment of the bacteria in external fields there is some evidence for non-thermal fluctuations, as the alignment could be described by an elevated effective temperature [37, 38].

More importantly, for a chain of magnetic particles without a stabilizing filament, the linear configuration is not the configuration of lowest energy. Rather, such a chain can be closed to a ring configuration, as seen experimentally [17]. Such rings have lower energy than straight chains for chains of four or more particles, so one can imagine them forming even despite the confinement in an elongated cell which should provide some stabilization to the linear configuration. Of course, closure of a ring is detrimental for the function of the chain, as the ring has no net magnetic moment. As a result of our analysis, we think that one of the roles of the filament is to stabilize the linear configuration against ring closure. That such stabilization is needed is suggested by observations of clusters of magnetosomes in mutants lacking the MamJ protein that links the magnetosomes to the filament (the situation is less clear for mutants lacking the filament protein MamK, as these cells exhibits multiple short linear chains). For a single actin-like filament, such stabilization is likely kinetic, i.e. by the increase of the barrier between the straight and ring configurations. For small bundles of such filaments, we expect the stabilization to be thermodynamic, i.e., in these cases, the linear configuration corresponds to the global energy minimum. Unfortunately, the finer internal structure of the magnetosome filament remains to be resolved and it also remains a possibility that some aspects of chain stability are different in different species of magnetotactic bacteria.

Appendix

In this appendix, we describe the calculation of the magnetic bending rigidity in more details. To evaluate the interaction energy, we express the angles between the dipole moments and between dipoles and their distance in terms of ϕ and θ,

$$\begin{aligned} \angle(m_i, m_j) &= |i-j|\,\varphi, \\ \angle(m_i, r_{ij}) &= \theta - \frac{(|i-j|-1)}{2}\varphi, \\ \angle(m_j, r_{ij}) &= \theta + \frac{(|i-j|+1)}{2}\varphi. \end{aligned} \tag{13}$$

Likewise, the distances r_{ij} are expressed as

$$r_{ij} = 2R\sin\frac{|i-j|\,\varphi}{2}. \tag{14}$$

For the moment, let us consider only nearest-neighbor interactions. In that case, the above expressions lead to the energy

$$E^{\mathrm{nn}}(\varphi, \theta) = -N\epsilon\,(1 - 1/N) \times (3\cos(2\theta + \varphi) + \cos\varphi). \tag{15}$$

In the equilibrium state, the orientation of the dipoles is such that the energy is minimal, thus we determine θ as a function of φ and thus of the chain curvature, by minimizing the energy. This leads to $\theta = -\varphi/2$, i.e. the magnetic dipoles orient in tangential direction with respect to the curvature circle, the tangential orientation is also valid for more general shapes of chains of magnetic dipoles as shown recently in [51]. In this case, the energy is given by

$$E^{\mathrm{nn}} = -N\epsilon\,(1 - 1/N) \times (3 + \cos\varphi). \tag{16}$$

In this equation, φ is a function of the curvature, l/R. Next, we use the Taylor expansion for small curvature, and express the energy as

$$E^{\mathrm{nn}} \approx -N\epsilon\left(1-\frac{1}{N}\right)+\frac{1}{8}N\epsilon\left(1-\frac{1}{N}\right)\left(\frac{l}{R}\right)^2. \tag{17}$$

Here the first term is the linear chain energy and the second term represents the contribution from bending with a magnetic bending rigidity of

$$\kappa_{\mathrm{magn}}^{\mathrm{nn}} = \frac{\epsilon l}{4}\left(1-\frac{1}{N}\right). \tag{18}$$

The same calculation can be done when including all magnetic interactions, i.e. beyond nearest neighbors. In that case, the energy is given by

$$E_{\mathrm{magn}}(\theta,\varphi) = -N\epsilon\sum_{n=1}^{N-1}\frac{(1-n/N)}{4\left(\frac{\sin(n\varphi/2)}{\sin(\varphi/2)}\right)^3}(3\cos(2\theta+\varphi)+\cos(n\varphi)). \tag{19}$$

Minimization of the energy again leads to the tangential orientation of the magnetic dipoles with $\theta = -\varphi/2$ and to the energy

$$E_{\mathrm{magn}} = -N\epsilon\sum_{n=1}^{N-1}\frac{(1-n/N)}{4\left(\frac{\sin(n\varphi/2)}{\sin(\varphi/2)}\right)^3}(3+\cos(n\varphi)). \tag{20}$$

The expansion for small curvature leads to

$$\begin{aligned} E_{\mathrm{magn}} &\approx -N\epsilon\times\left(1-\frac{1}{2}\left(\frac{l}{2R}\right)^2\right)\sum_{n=1}^{N-1}\frac{(1-n/N)}{n^3}+\cdots \\ &= E_{\mathrm{lin}}\left(1-\frac{1}{2}\left(\frac{l}{2R}\right)^2\right), \end{aligned} \tag{21}$$

with the energy E_{lin} of the linear chain given by equation (4) and the magnetic bending rigidity

$$\kappa_{\mathrm{magn}} = \frac{\epsilon l}{4}\sum_{n=1}^{N-1}\frac{(1-n/N)}{n^3} \approx \frac{\epsilon l}{4}\zeta(3) \simeq 0.3\epsilon l. \tag{22}$$

References

[1] Alberts B, Johnson A, Lewis J, Raff M, Roberts K and Walter P 2002 *Molecular Biology of the Cell* 4th edn (New York: Garland Science)
[2] Gitai Z 2005 *Cell* **120** 577
[3] Theriot J A 2013 *BMC Biol.* **11** 119
[4] Faivre D and Schüler D 2008 *Chem. Rev.* **108** 4875
[5] Bazylinski D A and Frankel R B 2004 *Nat. Rev. Microbiology* **2** 217
[6] Scheffel A, Gruska M, Faivre D, Linaroudis A, Plitzko J M and Schüler D 2006 *Nature* **440** 110
[7] Komeili A, Li Z, Newman D K and Jensen G J 2006 *Science* **311** 242
[8] Lohße A, Borg S, Raschdorf O, Kolinko I, Tompa E, Pósfai M, Faivre D, Baumgartner J and Schüler D 2014 *J. Bacteriology* **196** 2658
[9] Murat D, Falahati V, Bertinetti L, Csencsits R, Körnig A, Downing K, Faivre D and Komeili A 2012 *Mol. Microbiology* **85** 684
[10] Frankel R B, Bazylinski D A, Johnson M S and Taylor B L 1997 *Biophys. J.* **73** 994
[11] Lefèvre C T, Bennet M, Landau L, Vach P, Pignol D, Bazylinski D A, Frankel R B, Klumpp S and Faivre D 2014 *Biophys. J.* **107** 527
[12] De Gennes P G and Pincus P A 1970 *Phys. Kondens. Mater.* **11** 189
[13] Tlusty T and Safran S A 2000 *Science* **290** 1328
[14] Cebers A 2005 *Curr. Opin. Colloid Interface Sci.* **10** 167
[15] Yuan J, Xu Y and Müller A H E 2011 *Chem. Soc. Rev.* **40** 640
[16] Dreyfus R, Baudry J, Roper M L, Fermigier M, Stone H A and Bibette J 2005 *Nature* **437** 862
[17] Philipse A P and Maas D 2002 *Langmuir* **18** 9977
[18] Katzmann E, Müller F D, Lang C, Messerer M, Winklhofer M, Plitzko J M and Schüler D 2011 *Mol. Microbiology* **82** 1316
[19] Klumpp S and Faivre D 2012 *PLoS One* **7** e33562
[20] Koernig A, Dong J, Bennet M, Widdrat M, Andert J, Mueller F D, Schueler D, Klumpp S and Faivre D 2014 *Nano Lett.* **14** 4653
[21] Shcherbakov V P, Winklhofer M, Hanzlik M and Petersen N 1997 *Eur. Biophys. J. Biophys. Lett.* **26** 319
[22] Alphandéry E, Ding Y, Ngo A T, Wang Z L, Wu L F and Pileni M P 2009 *ACS Nano* **3** 1539
[23] Katzmann E, Scheffel A, Gruska M, Plitzko J M and Schüler D 2010 *Mol. Microbiology* **77** 208
[24] Messina R, Khalil L A and Stankovic I 2014 *Phys. Rev.* E **89** 011202(R)
[25] Shcherbakov V P and Winklhofer M 2004 *Phys. Rev.* E **70** 061803
[26] Wei A, Kasama T and Dunin-Borkowski R E 2011 *J. Mater. Chem.* **21** 16686
[27] Xiong Y, Ye J, Gu X and Chen Q-W 2007 *J. Phys. Chem.* C **111** 6998
[28] Li S P, Peyrade D, Natali M, Lebib A, Chen Y, Ebels U, Buda L D and Ounadjela K 2001 *Phys. Rev. Lett.* **86** 1102
[29] Stoz J F, Chang S B R and Kirschvink J L 1986 *Nature* **321** 849
[30] Goubault C, Jop P, Fermigier M, Baudry J, Bertrand E and Bibette J 2003 *Phys. Rev. Lett.* **91** 260802
[31] Biswal S L and Gast A P 2003 *Phys. Rev.* E **68** 021402

[32] Landau L D, Lifshitz E M, Kosevich A M and Pitaevskii L P 1986 *Theory of Elasticity* vol 7 3rd edn (Oxford: Pergamon)
[33] Jogler C and Schüler D 2013 *Proc. R. Soc.* A **63** 501
[34] Barrat J L and Joanny J F 1996 *Adv. Chem. Phys.* **94** 1
[35] Vella D, du Pontavice E, Hall C L and Goriely A 2014 *Proc. R. Soc.* A **470** 20130609
[36] Rubinstein M and Colby R H 2003 *Polymer Physics* (Oxford: Oxford University Press)
[37] Zhu X, Ge X, Li N, Wu L-F, Luo C, Ouyang Q, Tu Y and Chen G 2014 *Integr. Biol. (Camb.)* **6** 706
[38] Nadkarni R, Barkley S and Fradin C 2013 *PLoS One* **8** e82064
[39] Usov N A, Fdez-Gubieda M L and Barandiaran J M 2013 *J. Appl. Phys.* **113** 023907
[40] Jogler C *et al* 2010 *Environ. Microbiology* **12** 2466
[41] Bean C P and Livingston J D 1959 *J. Appl. Phys.* **30** S120
[42] Chantrell R W, Bradbury A, Popplewell J and Charles S W 1980 *J. Phys. D: Appl. Phys.* **13** L119
[43] Wen W J, Kun F, Pal K F, Zheng D W and Tu K N 1999 *Phys. Rev.* E **59** R4758
[44] Lavender H B, Iyer K A and Singer S J 1994 *J. Chem. Phys.* **101** 7856
[45] Vandewalle N and Dorbolo S 2014 *New J. Phys.* **16** 013050
[46] Tripp S L, Dunin-Borkowski R E and Wei A 2003 *Angew. Chem., Int. Ed. Engl.* **42** 5591
[47] Yanagida T, Nakase M, Nishiyama K and Oosawa F 1984 *Nature* **307** 58
[48] Gittes F, Mickey B, Nettleton J and Howard J 1993 *J. Cell Biol.* **120** 923
[49] Ott A, Magnasco M, Simon A and Libchaber A 1993 *Phys. Rev.* E **48** R1642
[50] Claessens M M A E, Bathe M, Frey E and Bausch A R 2006 *Nat. Mater.* **5** 748
[51] Hall C L, Vella D and Goriely A 2013 *SIAM J. Appl. Math.* **73** 2029